

ADVANCED DIGITAL SIGNAL PROCESSING FOR EFFECTIVE BEAM POSITION MONITORING

D. Liakin, ITEP, Moscow, Russia
 K. Lang, P. Forck, R. Singh, GSI, Darmstadt, Germany

Abstract

The latest experiences in digital signal processing of BPM data obtained at the synchrotrons of ITEP and GSI are discussed. The data from the ITEP was collected by a BPM processor prototype while the SIS18 BPM DAQ (GSI) uses an already renovated digital system. Due to the different concept of BPM architectures on those facilities it is possible to compare algorithms oriented to certain hardware. Several algorithms of position detection are compared to each other.

HARDWARE

Modern signal processors used in beam position monitoring look today pretty similar. The proton and heavy ion cycling accelerators operate on relatively low frequencies and use the digital processing from very beginning stages of BPM data flow.

The beam position monitoring system of SIS 18 (GSI), shown in Fig. 1, has a classical digital BPM setup. It is based on modules with four analogue input channels, a powerful FPGA and a single board computer (SBC) for remote setup. Modules are independent and supervision function is an option of the host computer.

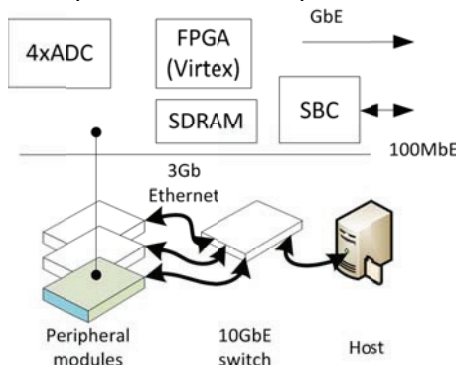


Figure 1: Modernized BPM processor structure of SIS 18 (GSI).

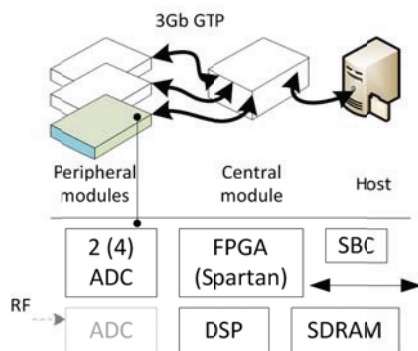


Figure 2: Base station prototype structure and proposed BPM configuration for U10 (ITEP).

Figure 2 presents a prototype module and a possible system configuration for the future ITEP synchrotron and storage ring BPM systems. The leak of performance of the budgetary FPGA is compensated by using of a two-core DSP and a high performance low-cost and low-overhead 3Gbps serial connection to delegate some data operation into the next hardware level.

POSITION DECODING

The main purpose of BPMs is position decoding. The input data from ADCs today is usually significantly oversampled and data reduction is desirable already on the beginning stage. There are few possibilities to convert ADC samples into the rarefied position related data.

A common algorithm presently used in BPMs is the digital interpretation of the former analogue prototype – base line restoration and window integration.

$$A = \int_{t_0}^{t_1} w(t)(U(t) - B)dt \quad (1)$$

The advantage of this algorithm is an invariance of an integral in the case of constant w . The second algorithm we tested is based on signal power estimation.

$$A = \sqrt{\int_{t_0}^{t_1} U(t)^2 dt} \quad (2)$$

This simple formula even does not include any parameters for adjustment. Nevertheless in certain condition it shows better result than the classical one. It is essential also to use spectral components of a signal:

$$A_n = \|\dot{A}_n\| \quad \dot{A}_n = \int_{t_0}^{t_1} U(t)e^{j2\pi nt/T} dt \quad (3)$$

In the simplest case only the first harmonic is used. Involving a full signal frequency spectrum with uniform weight coefficients for position calculation will be equivalent to Eq. 2.

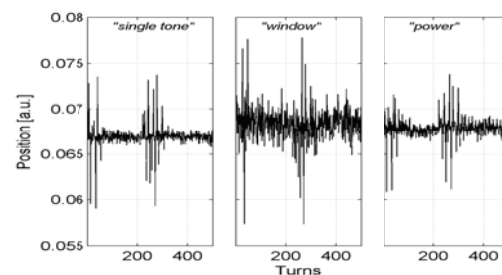


Figure 3: Same BPM data decoded with different algorithms.

Figure 3 shows position calculated with these three algorithms. The single tone looks preferable over others regarding the lowest noise. To get a better result one may use the second, third and next tones of the signal spectra. However, a multi-tone operation must be used with care. As shown in Fig. 4, due to the frequency dependence, additional signals may introduce an offset in position measurements.

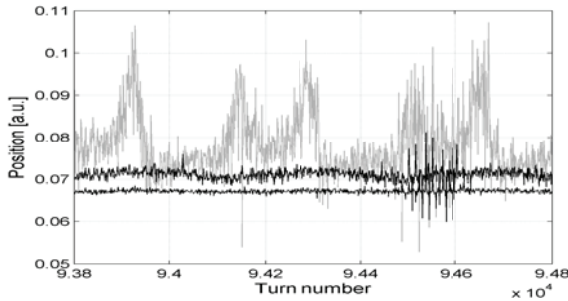


Figure 4: Position data obtained separately for main, second and third tones.

ERROR SOURCES IN BPM

Generally the accuracy of position measurements is limited with fundamental values which are stochastic, have no structure and thus could not be withdrawn from the system. An example is the noise of a preamplifier. There are also elements which are not belonging to the system itself. Figure 5 shows a signal spectrum from a BPM electrode. There is a ‘human made’ component B, which is probably a result of interference of a short periodic external process. It is well dumped down to -60dB comparing to the first signal tone, but nevertheless it is a main contributor in the beam position measurement error, see also Fig. 3 and spurious spikes in Fig. 6.

The second discovered contributor is a crosstalk between longitudinal synchrotron oscillation and transversal beam position. It is not visible on the spectrum shown in Fig. 5 due to the different frequency domain. Effect is shown in Fig. 6 where one can see a correlation between longitudinal movement and measurements of transversal position. The most reasonable explanation is, probably, a nonlinearity of the analogue part of electronics.

BUNCH CYCLE RECONSTRUCTION

Position decoding algorithms are sensitive to the integration limits t_0 and t_1 in Eqs. 1 to 3, and the BPM electronics must implement some algorithms to recover the bunch frames. Using a well determined signal like accelerating RF field would be the best solution, but in many cases the electronic does not provide an additional digitized analog input and the only way is to use a signal from the BPM itself. Figures 7 and 8 show some possibilities for the bunch separation.

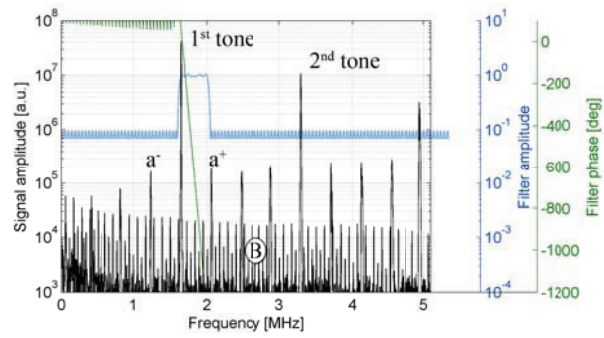


Figure 5: Signal spectrum of the SIS 18 BPM, and Bode diagram of the carrier reconstruction bandpass filter.

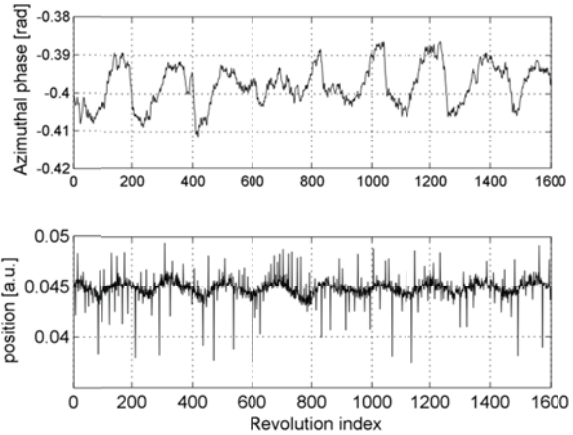


Figure 6: Synchrotron azimuthal oscillations (top) and their trace on radial position data

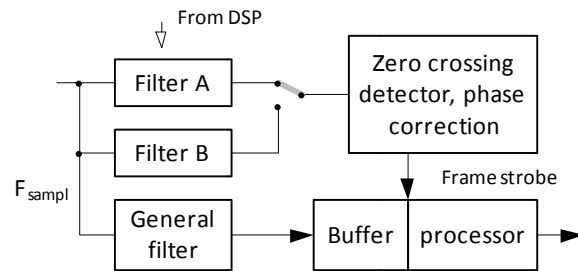


Figure 7: Precise signal period reconstruction by dynamically loading bandpass filters.

In Fig. 7 the system uses a set of dynamically loaded bandpass filters to purify the main tone of a beam signal. Filter’s passbands are overlapped to smoothly cover the whole frequency range. Stopbands are chosen to suppress the bunch-to-bunch modulation frequencies a^+ and a^- (Fig. 5).

Figure 8 shows another way for bunch cycle reconstruction. A numerically controlled oscillator and digital mixer shift the signal frequency into the passband of the low-pass filter LPF, while the second mixer moves it back. Though the LPF in Fig. 8 is implemented as a multirate filter, the sampling rate on its output is exactly the same as the system sampling rate (those of ADCs). Depending on algorithm this scheme operates as a phase locked loop (PLL) or as a frequency tracking device.

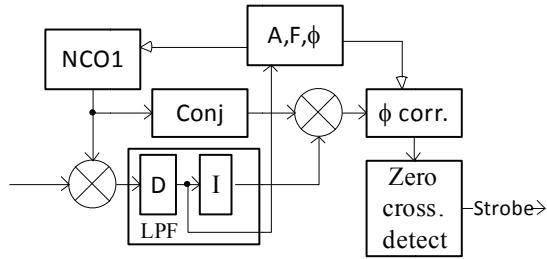


Figure 8: Signal period reconstruction using NCO.

MULTIPLE SIGNAL SOURCES

Figure 4 is an example of a situation when the beam position could be obtained in several ways. The number of free variables is less than the number of equations. Every signal harmonic, or combination of harmonics provide their own beam position value. The system is over-determined. The over-determination may come from signal spectra in frequency domain, multiple sampling points in time domain or from BPM construction, as shown in Fig. 9.

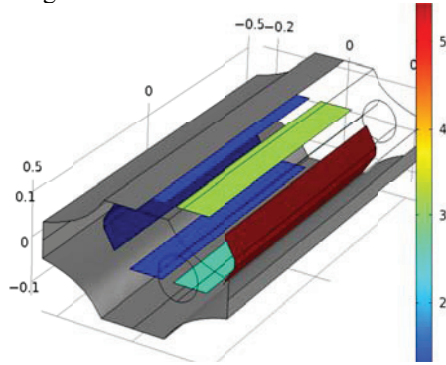


Figure 9: A six-pole BPM proposed for the FAIR collector ring. All six potentials must be used to optimize the signal to noise ratio for entire range of beam positions.

The fundamental idea is that every new portion of data improves our knowledge about the subject. But as one can see from Fig. 4 the new data introduce also some noise and wrong balance between data may lead more noisy output. As a result of improper data, merging the full spectrum “power” algorithm in Fig. 3 issued more noisy position than the “single tone” competitor. In general, mentioned above over-determined system could be extended to a determined state by introduction weighting coefficients w_i as new free variables and including new constrains in form of the problem of minimization of the statistical error distribution function $\delta(w_1, \dots, w_n)$. Excluding constrains the linearized equation is:

$$X + \delta(w_1, \dots, w_n) = \sum (K_i A_i + \varepsilon_i) w_i + X_0;$$

$$\sum w_i = 1.$$

With non-correlated Gaussian noise:

$$X + \delta(w_1, \dots, w_n) = X_0 + \sum K_i A_i w_i + \varepsilon;$$

$$\varepsilon = \sqrt{\sum (w_i \varepsilon_i)^2}.$$

The minimal error value of $\varepsilon = \varepsilon_{min}$ is achieved when

$$w_n = \frac{\sum_{i \neq n} \varepsilon_i^2}{\sum \varepsilon_i^2} \frac{n}{n-1}.$$

In the case of two variables:

$$\varepsilon_{min} = \frac{\varepsilon_1 \varepsilon_2}{\sqrt{\varepsilon_1^2 + \varepsilon_2^2}}; \quad \varepsilon_m / \sqrt{2} \leq \varepsilon_{min} \leq \varepsilon_m.$$

where ε_m is a lowest from ε_1 and ε_2 . Looking at Fig. 4, the improvement in signal-to-noise ratio would be in the range of 5% for dual tone operation, but for shorter bunches the effect would be more appreciable.

Figure 9 shows a BPM construction, optimized for low current application with antiproton beam in the collector ring of FAIR. The over-determined system of signals is essential feature of this BPM. There the position detection algorithm is obviously not linear, and weight coefficients w_i are not constant but depending on measured beam position. Figure 10 compares the simulated position noise of six-pole and linear cut BPM in the case of 10^8 antiprotons in the collector ring.

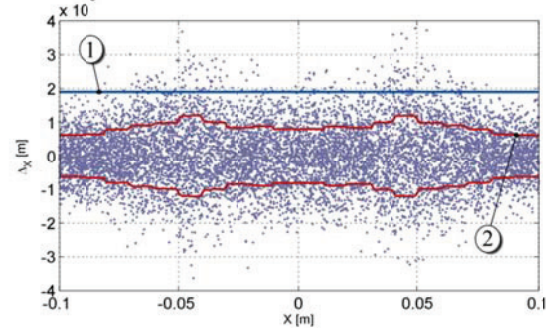


Figure 10: Standard deviation from actual value for position measurement with linear-cut (1) and six-pole (2) BPMs.

CONCLUSION

A new generation of beam position monitors shows an excellent performance for standard applications like closed orbit measurements. Nevertheless, there are still certain ways to improve their performance which could be an interest in special cases of operation – low beam current, tune measurements etc. In many cases better performance could be achieved without changing the hardware, only by using more sophisticated algorithms. However, it was found that using a general purpose DSP is very helpful on the algorithms design and test stage as well as for routine system monitoring.

REFERENCES

- [1] K. Lang et al., Performance test of digital signal processing for GSI synchrotron BPMS. Proc. Of PCaPAC08, Ljubljana, Slovenia.
- [2] A. Galatis et al., Digital beam position measurement at GSI-SIS and CERN-PS. Proc. Of DIPAC 2005, Lyon, France.
- [3] S. Stergiopoulos (Editor), Advanced signal processing handbook, CRC Press LLC, 2001.